Janus GroupV1B-Based Pnictogen-Halide Monolayers: A New Class of Multifunctional Quantum Materials from First-Principles Predictions

Sergey Gusarov[1], Chinedu E. Ekuma[2], Gap Soo Chang[3], Mina Alizade[4], Mosayeb Naseri[1,5*]

[1]Digital Technologies Research Centre, National Research Council Canada, 1200 Montreal Road, Ottawa, Ontario K1A0R6, Canada
[2]Department of Physics, Lehigh University, Bethlehem, Pennsylvania 18015, USA
[3]Department of Physics and Engineering Physics, University of Saskatchewan, Saskatoon, SK S7N5E2, Canada
[4]Department of Materials Engineering, Science and Research Branch, Islamic Azad University, Tehran, Iran
[5]Department of Chemistry, Department of Physics and Astronomy, CMS – Center for Molecular Simulation, IQST – Institute for Quantum Science and Technology, Quantum Alberta, University of Calgary, 2500 University Drive NW, Calgary, Alberta, Canada, T2N 1N4

Emails: *mosayeb.naseri@nrc-cnrc.gc.ca; mosayeb.naseri@ucalgary.ca*

Supplementary Discussion 1: Solar-to-hydrogen (STH) efficiency

STH efficiency is estimated by the product of the efficiency of light absorption η_{abs} and charge carrier utilization η_{cu} using the following expression[1]:

$$\eta_{STH} = \eta_{abs} \times \eta_{cu} \times \frac{\int_0^\infty P(\hbar\omega)d(\hbar\omega)}{\int_0^\infty P(\hbar\omega)d(\hbar\omega) + \Delta\Phi\int_{E_g}^\infty \frac{P(\hbar\omega)}{\hbar\omega}d(\hbar\omega)} \quad \text{(S1)}$$

where $\Delta\Phi$ is the electrostatic potential difference.

The efficiency of light absorption is defined as:

$$\eta_{abs} = \frac{\int_{E_g}^\infty P(\hbar\omega)d(\hbar\omega)}{\int_0^\infty P(\hbar\omega)d(\hbar\omega)} \quad \text{(S2)}$$

where E_g is the band gap of photocatalyst and $P(\hbar\omega)$ is the AM1.5 solar energy flux at the photon energy $\hbar\omega$.

The charge carrier utilization efficiency(η_{cu}) is estimated by

$$\eta_{cu} = \frac{\Delta G\int_E^\infty \frac{P(\hbar\omega)}{\hbar\omega}d(\hbar\omega)}{\int_{E_g}^\infty P(\hbar\omega)d(\hbar\omega)} \quad \text{(S3)}$$

where ΔG is the potential difference for water splitting (1.23 eV) and *E* is the energy of photons that can be used for water splitting, which can be defined as

$$E = \begin{cases} E_g, (\chi(H_2) \geq 0.2,\ \chi(O_2) \geq 0.6) \\ E_g + 0.2 - \chi(H_2), (\chi(H_2) < 0.2,\ \chi(O_2) \geq 0.6) \\ E_g + 0.6 - \chi(O_2), (\chi(H_2) \geq 0.2,\ \chi(O_2) < 0.6) \\ E_g + 0.8 - \chi(H_2) - \chi(O_2), (\chi(H_2) < 0.2,\ \chi(O_2) < 0.6) \end{cases} \quad \text{(S4)}$$

where $\chi(H_2)$ and $\chi(O_2)$ are the overpotentials of the H_2 (HER) and O_2 (OER) evolution

reactions, respectively. Considering the energy loss during carrier migration between different materials, the required over potentials for HER and OER are assumed to be 0.2 and 0.6 eV, respectively.

Reference

1. Fu, C. F.; Sun, J.; Luo, Q.; Li, X.; Hu, W.; Yang, J. Intrinsic Electric Fields in Two-dimensional Materials Boost the Solar-to-Hydrogen Efficiency for Photocatalytic Water Splitting. Nano Lett. **2018**, 18, 6312.

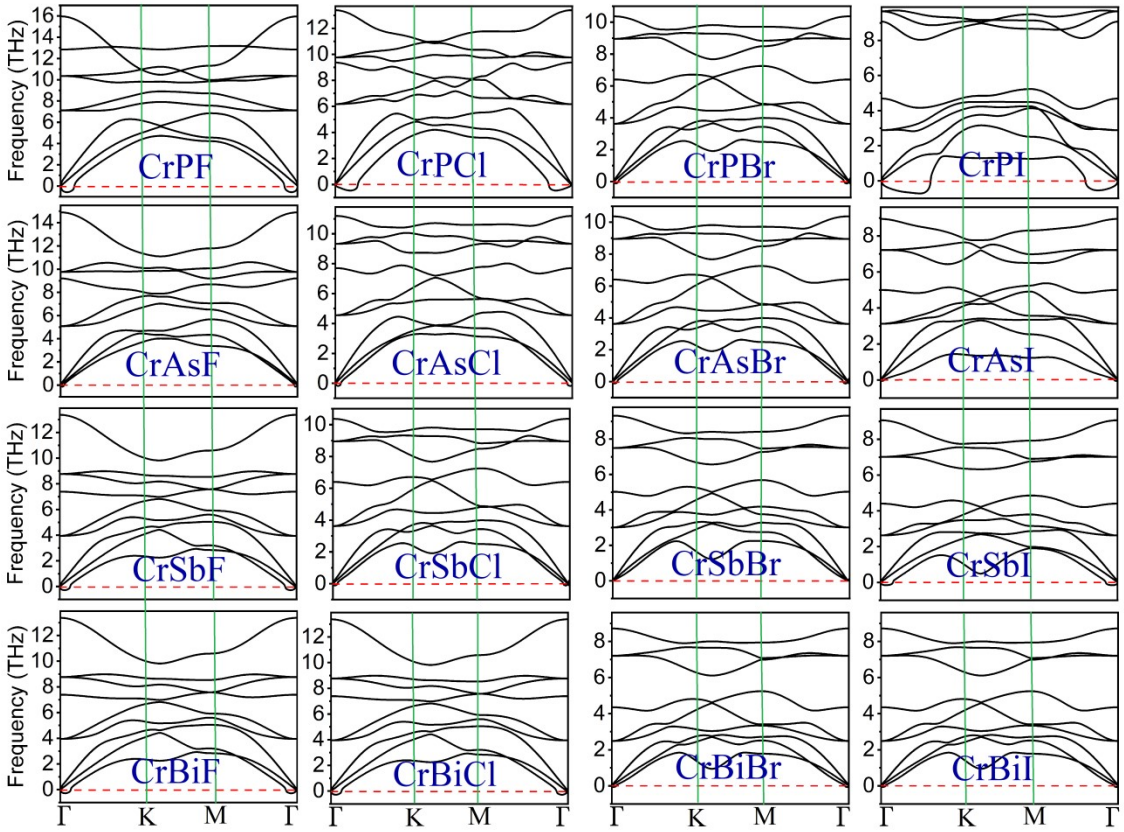

Figure S1. The phonon dispersion spectra of 2D Janus CrXY monolayer structures.

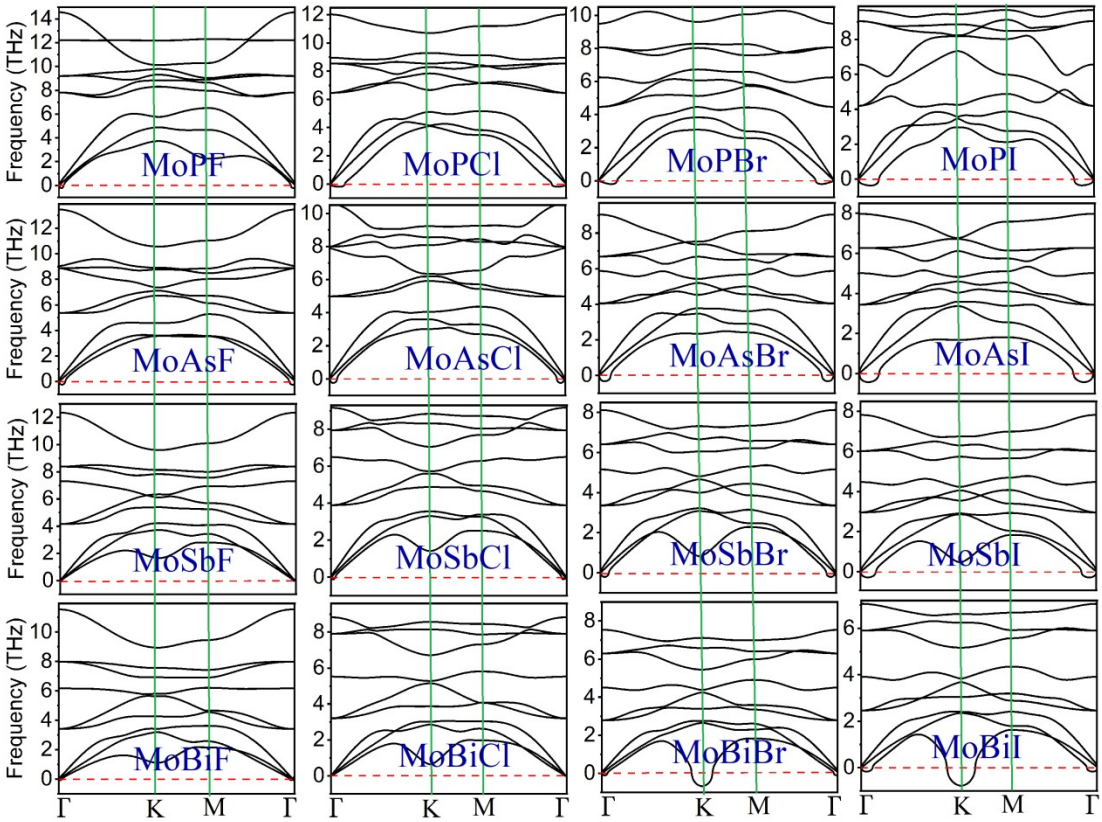

Figure S2. The phonon dispersion spectra of 2D Janus MoXY monolayer structures.

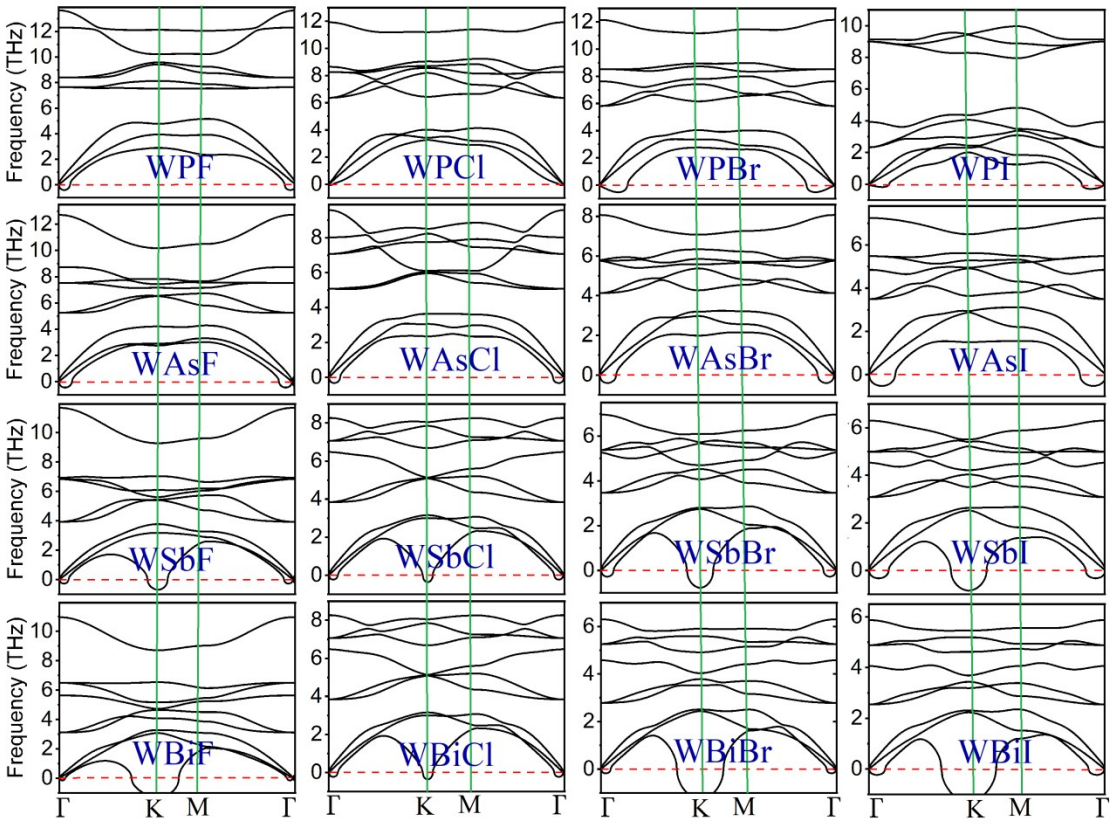

Figure S3. The phonon dispersion spectra of 2D Janus WXY monolayer structures.

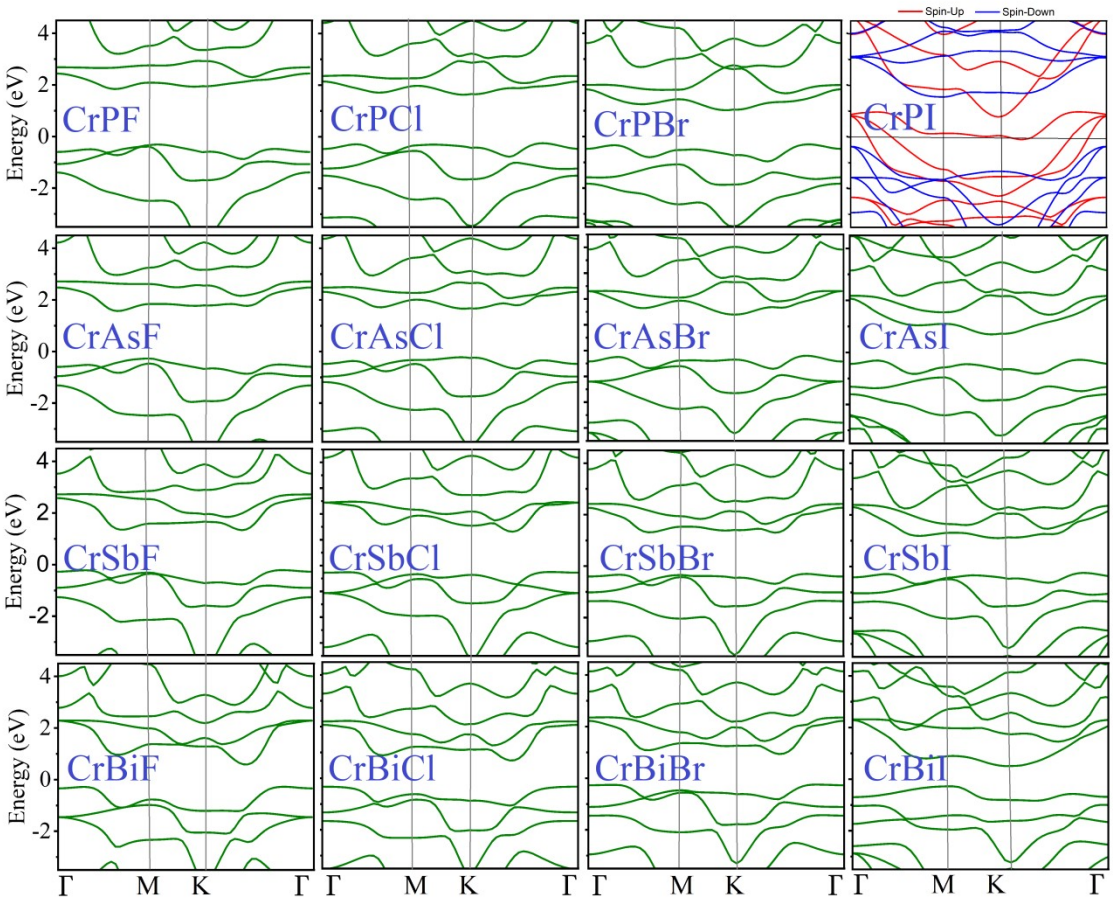

Figure S4. The band structures for 2D Janus CrXY monolayer structures calculated with HSE06 functional.

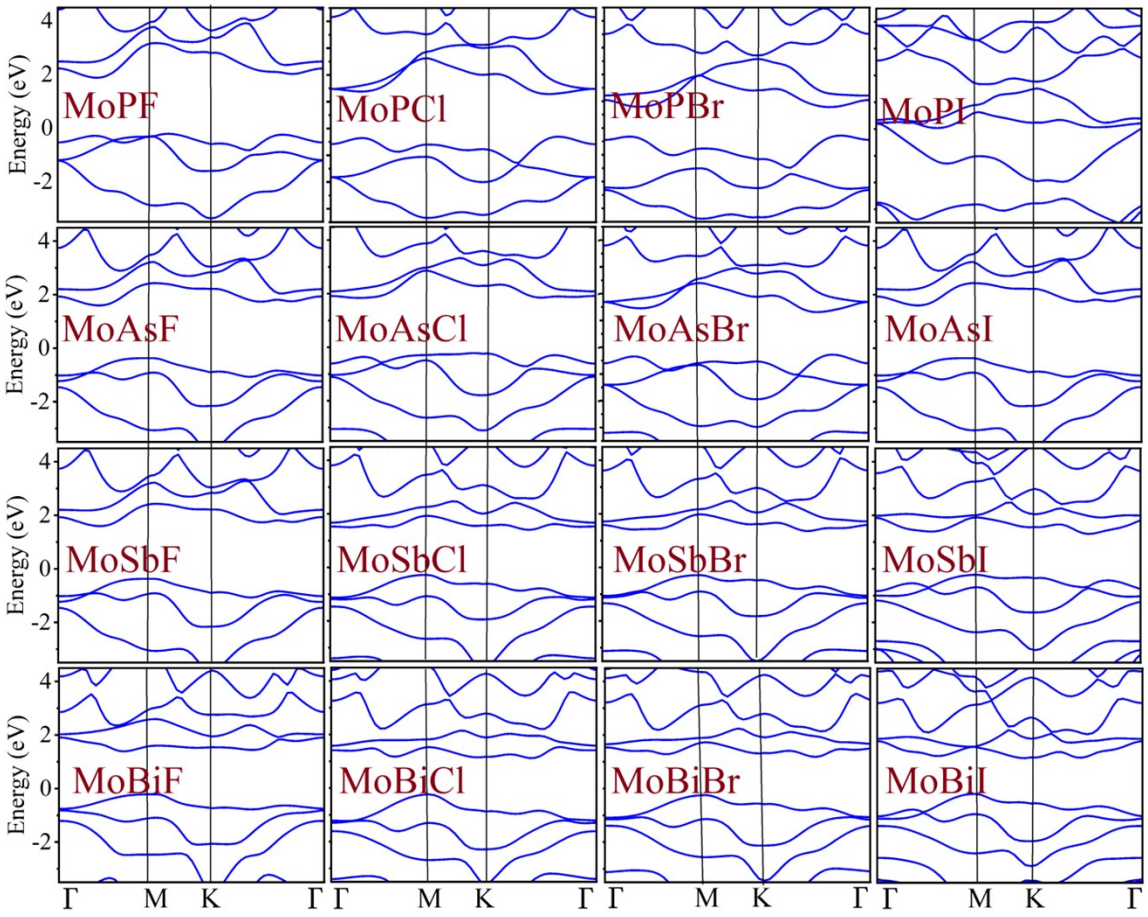

Figure S5. The band structures for 2D Janus MoXY monolayer structures calculated with HSE06 functional.

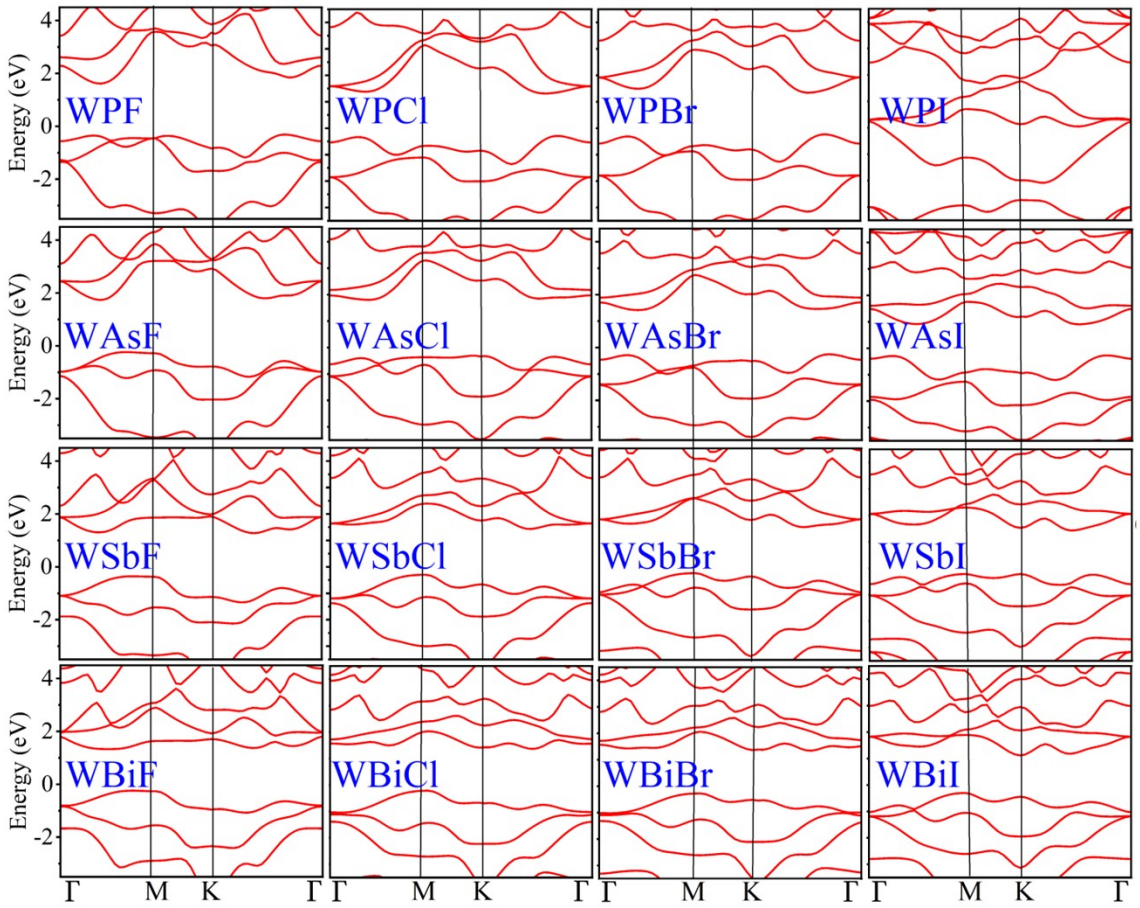

Figure S6. The band structures for 2D Janus WXY monolayer structures calculated with HSE06 functional.

Table S1. Electrostatic potential difference ΔΦ (eV), work function Φ (eV) on the $(00\bar{1})$, and (001) sides.

Monolayer	Φ $(00\bar{1})$ (eV)	Φ (001) (eV)	ΔΦ (eV)
CrPF	5.456	6.028	0.572
CrPCl	3.997	6.13	2.133
CrPBr	3.495	5.988	2.493
CrPI	3.806	4.97	1.164
CrAsF	5.244	5.158	0.086
CrAsCl	4.124	5.548	1.424
CrAsBr	3.573	5.52	1.947
CrAsI	3.137	5.477	2.34
CrSbF	4.981	4.44	0.541
CrSbCl	3.941	4.62	0.679

CrSbBr	3.558	4.787	1.229
CrSbI	3.334	5.044	1.71
CrBiF	4.845	3.878	0.967
CrBiCl	4.061	4.091	0.03
CrBiBr	3.712	4.21	0.498
CrBiI	3.463	4.42	0.957
MoPF	5.12	6.299	1.179
MoPCl	3.691	6.009	2.318
MoPBr	3.337	5.803	2.466
MoPI	5.839	5.143	0.696
MoAsF	4.94	5.527	0.587
MoAsCl	4.013	5.738	1.725
MoAsBr	3.355	5.528	2.173
MoAsI	2.922	5.454	2.532
MoSbF	4.691	4.751	0.06
MoSbCl	3.861	4.937	1.076
MoSbBr	3.572	5.138	1.566
MoSbI	3.163	5.147	1.984
MoBiF	4.458	3.974	0.484
MoBiCl	3.735	4.063	0.328
MoBiBr	3.462	4.269	0.807
MoBiI	3.153	4.37	1.217
WPF	4.818	6.268	1.45
WPCl	3.422	6.055	2.633
WPBr	2.662	6.048	3.386
WPI	3.128	4.887	1.759
WAsF	4.644	5.452	0.808
WAsCl	3.72	5.741	2.021
WAsBr	3.224	5.622	2.398
WAsI	2.699	5.364	2.665
WSbF	4.35	4.532	0.182
WSbCl	3.49	4.843	1.353
WSbBr	3.368	5.159	1.791
WSbI	3.135	5.264	2.129
WBiF	4.191	3.756	0.435
WBiCl	3.49	4.062	0.572
WBiBr	3.185	4.181	0.996
WBiI	2.972	4.32	1.348